

High-throughput sorting of two-color fluorescent-labeled zebrafish embryos

Hongzhen Tang*, Linbo Wang[†], Xiaohu Chen[†],
Chong Chen[†], Hui Li*,[†] and Guang Yang^{†,‡}

**Changchun University of Science and Technology
Changchun, Jilin 130022, P. R. China*

[†]*Jiangsu Key Laboratory of Medical Optics
Suzhou Institute of Biomedical Engineering and Technology
Chinese Academy of Sciences,
Suzhou, Jiangsu 215163, P. R. China*
†yangg@sibet.ac.cn

Received 17 October 2022

Accepted 15 December 2022

Published 16 February 2023

The zebrafish embryos were widely employed in genetics, development and drug discovery studies as miniaturized animal models. Sorting of two-color fluorescent embryos is often required in large-scale experiments but it is challenging to manually sort with high efficiency. Here, we reported a high-throughput sorting system for two-color fluorescent zebrafish embryos. The embryos can be automatically loaded from a sample pool and sorted based on the average fluorescent intensity. The two-color fluorescent signals were split into two lines and detected by an area array camera. The system achieves the sorting of 100 embryos in less than 10 min with an accuracy of greater than 95%.

Keywords: High-throughput; zebrafish embryo; two-color sorting; automatic.

1. Introduction

The zebrafish is an excellent animal model for studying human disease, with 80% gene similar to humans.^{1–4} Due to advantages such as small size, ease of raising, and regular spawning, zebrafish are also preferred for large-scale experiments which are crucial for the morphological and phenotypic characterization.^{5–10} The sorting of different types of

zebrafish embryos is a prerequisite for large-scale experiments. Currently, the sorting was conducted manually under a traditional microscope, which is slow and labor intensive.^{11,12} Especially, sorting two-color fluorescent-labeled embryos is very tricky because it requires frequent switching of fluorescent filter wheels back and forth. Therefore, for the extensive sorting of two-color fluorescent zebrafish

*Corresponding author.

This is an Open Access article. It is distributed under the terms of the Creative Commons Attribution 4.0 (CC-BY) License. Further distribution of this work is permitted, provided the original work is properly cited.

embryos, a high-throughput sorting device is required.^{13–18}

Flow cytometer is typically used in cell biology to automatically filter cells at high-throughput but it cannot be applied to zebrafish embryos with millimeter size. The Complex Object Parametric Analyzer and Sorter invented by Union Biometrica can screen of miniature model animals with sizes ranging from $10\text{ }\mu\text{m}$ to $1500\text{ }\mu\text{m}$. Yaniks developed a Vertebrate Automated Screening Technology (VAST) system that enables the automatic loading, positioning, and rotating of zebrafish embryos under the commercial confocal system within 9.6 s.^{7,19} However, for sorting the zebrafish where imaging is not required, the VAST system is complicated and slow especially for two-color fluorescent-labeled zebrafish embryos.

In this paper, we developed a flow-based two-color zebrafish embryo sorting system that allows the automatic loading and sorting of zebrafish embryos. This system uses two-line images obtained by an area array camera to capture the fluorescent signals of zebrafish embryos flowing through a capillary. A Gaussian beam passed through a cylindrical lens to form light sheets as excitation light to illuminate the sample, reducing the exposure of light to the living embryos.²⁰ The system can sort each embryo within 20 s and the accuracy of the automatic sorting can reach above 95%. It can be upgraded to have additional detection channels to sort three- or four-colored label embryos.

2. Materials and Methods

2.1. Schematic diagram of two-color sorting system

The schematic of the flow-based two-color zebrafish embryos sorting system is shown in Fig. 1. A 488 nm and 561 nm fiber-coupled laser (Oxxius laser, L4CC-CSB-1315) was first collimated by objective (illumination objective (IO), Olympus, 10 \times , NA 0.25, Japan). Subsequently, the resulting beam was expanded by a scale of 3 with lens group L1 (LA1131-A, Thorlabs, USA) and L2 (LA1433-A, Thorlabs, USA). A cylindrical lens CL (GCL110118, Beijing Daheng Photo-Electric Technology Company, China) was used to focus the beam to the back focal plane of the IO/detection objective (DO) (Olympus, 10 \times , NA 0.25, Japan). As a result, a light sheet was created at the capillary where the zebrafish embryos flow. The fluorescence collected by the DO passed through a long-pass dichroic mirror DM1 and was split into two channels with dichroic mirror DM2 (DMLP550T, Thorlabs, USA). After being filtered by the corresponding filters F1 (MF630-69, Thorlabs, USA) and F2 (MF525-39, Thorlabs, USA), the split beams were recombined with dichroic mirror DM3 (DMLP550T, Thorlabs, USA). This allowed for the simultaneous capturing of two channel fluorescence using a single camera (Prime BSI, Teledyne Photometrics, USA) with lens L3 (LA1708-A, Thorlabs, USA). By adjusting the angles of the mirrors M1, M2 (BB2-E02-10, Thorlabs, USA), the emitted light can be focused on different positions of the camera target surface.

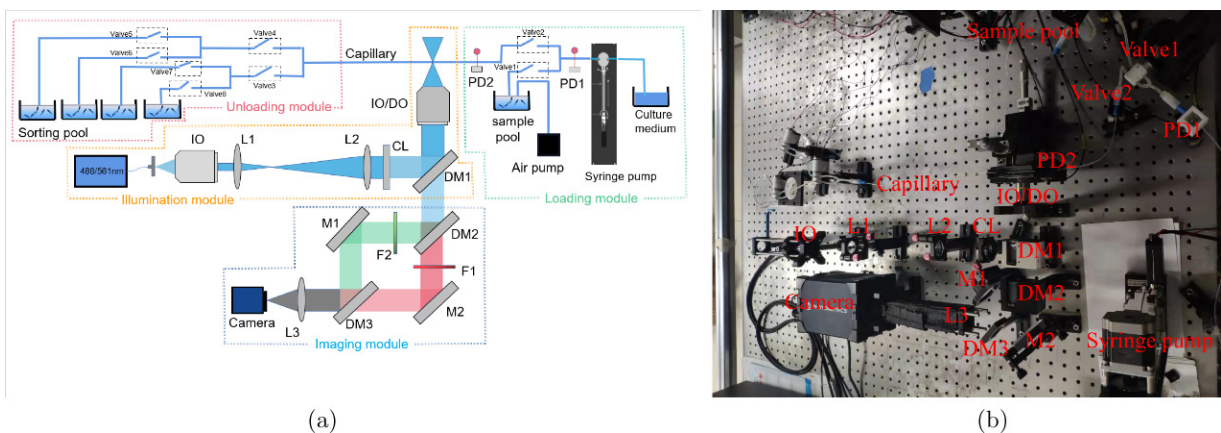


Fig. 1. Schematic diagram and real setup of the high-throughput sorting system. (a) Schematic diagram. (b) Real setup. IO: 10 \times objective lens, numerical aperture of 0.25. L1–L3: Lens. CL: Cylindrical lens. DM1: Dual-channel dichroic mirror. IO/DO: 10 \times objective lens, numerical aperture of 0.25. DM2 and DM3: Dichroic mirrors. F1 and F2: Fluorescence filters. M1 and M2: Mirrors. Camera: Area array camera. PD1 and PD2: Photodetectors.

The two-color fluorescence lines were projected onto the camera with a pixel number of 2048×2048 and a pixel size of $6.5\text{ }\mu\text{m} \times 6.5\text{ }\mu\text{m}$. Fluorescence image of each color covered 2048×6 pixels and was spaced with a spacing of 200 pixels. The exposure time was set to 10 ms to collect sufficient fluorescence signal.

A flow system was designed consisting of a loading and an unloading module. In the loading module, the embryos were transported by a syringe pump (SP60-1A, DK Infusetek Co., Ltd., China). The air pump was applied to prevent zebrafish embryos from gathering at the bottom of the sample pool. The embryos were detected as they passed through the photoelectric detectors (PD1, PD2, FS-N41N, Japan). The flow direction of embryos was transformed by the valve 1 and valve 2. In the unloading module, the embryos were sorted to the sorting pool by the three-way valve 3–4, 5–6, and 7–8.

2.2. Sorting procedure

At the beginning of each cycle, valve 1 of the loading module in Fig. 1 was opened and the air in the capillary was expelled. The embryos were lightly anesthetized before sorting. Zebrafish embryos in the sample pool were extracted by a syringe pump at a loading speed of 0.167 mL/s (332 mm/s). After the embryo was detected by a photoelectric detector (PD1), the syringe pump was changed to push mode with valve 2 opened and valve 1 closed, making the embryo flow into the imaging module at a speed of 0.083 mL/s (165 mm/s). After embryo detection by a photoelectric detector (PD2), the camera was triggered and the syringe pump was run at a lower speed of $0.25\text{ }\mu\text{L/s}$ (5 mm/s) to ensure high imaging quality. We chose a flow speed of about 2 mm/s resulting in 154 lines/mm which is adequate for sorting. The resulting imaging time $\sim 1\text{ s}$ per embryo, given that the length of 4–5 days post-fertilization (dpf) of zebrafish embryo is $\sim 2.5\text{ mm}$. According to the fluorescence signals, zebrafish embryos were sorted into four classes, namely, green, red, green/red, and nonlabeled. The sorted embryos were finally transported to four sorting pools by switching on valves 3–8. The high-throughput sorting system continuously repeats these steps and each cycle takes approximately within 20 s. The entire system is controlled by software written in Python.

2.3. Culture of zebrafish embryos

Wild-type and transgenic zebrafish (fli1a:EGFP, gata1a:DsRed) were used in all the experiments. One to two pairs of parent fish were placed in each box. The room light was set to a light and night/dark cycle of 14:10 h, to stimulate the zebrafish to lay eggs. The next morning, the septum was taken away and the inner baffle in the box was obliquely laid. This was primarily used to prevent the parent fish from eating the eggs. After waiting for 20 min, the female fish produced eggs and the eggs were collected in a culture dish. The zebrafish embryos were incubated at 28°C . The sundries and unfertilized embryos in the culture dish was suctioned by a dropper, to avoid causing the death of other embryos. After 24 h, configured $1 \times N$ -phenylthiourea was added to inhibit the generation of embryo pigment.

The zebrafish preparation processes were carried out in accordance with the Guide for the National Institutes of Health guide for the care and use of laboratory animals (NIH Publications No. 8023, revised 1978), and were approved by the animal ethics committee of Suzhou Institute of Biomedical Engineering and Technology, CAS.

3. Results and Discussion

3.1. System calibration with fluorescent spheres

To validate the length of the light sheet, we captured images of the green and red fluorescent-labeled spheres. The diluted fluorescent spheres were evenly coated on the cover slip and were captured by our system. Figure 2(a) shows an image of the green fluorescent-labeled sphere. The inner diameter of the capillary used was 0.8 mm and the light sheet completely covered the capillary. Figure 2(d) shows the gray value distribution of the straight line in Fig. 2(a). The 488 nm channel was about $130\text{ }\mu\text{m}$ thick. Figure 2(b) shows an image of the red fluorescent-labeled sphere. Figure 2(e) shows the gray value distribution of the straight line in Fig. 2(b). The full width at half maximum was 40 pixels. The 561 nm channel was $260\text{ }\mu\text{m}$ thick. Figure 2(c) shows an image of fluorescent spheres collected simultaneously by the two channels. Figure 2(f) shows the gray value distribution of the straight line in Fig. 2(c).

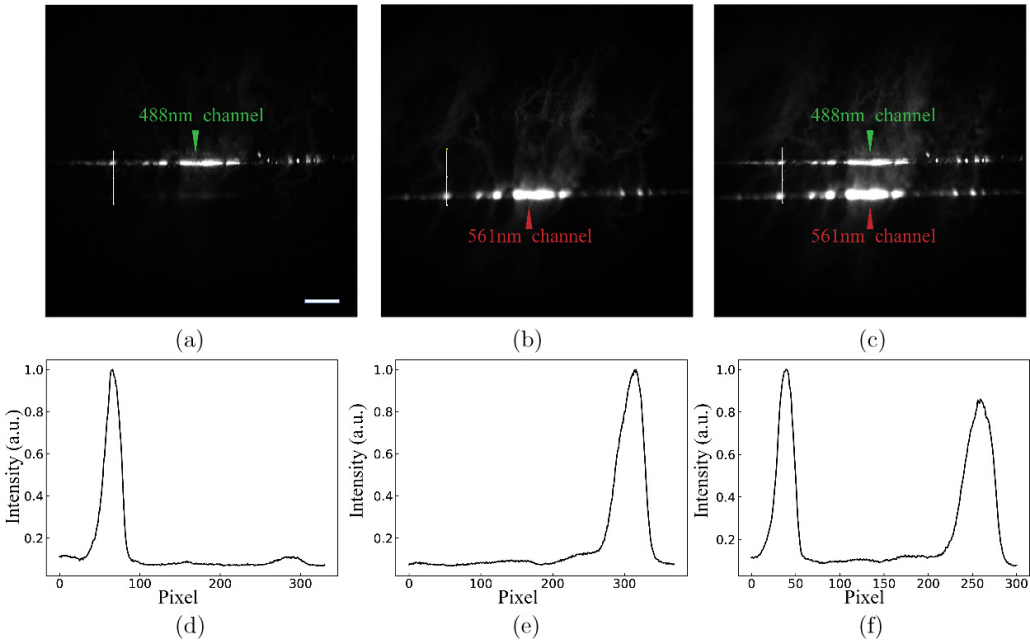


Fig. 2. Images of the fluorescent spheres captured by the two-color sorting system. (a) Image with green fluorescent spheres. Scale bar: 1.5 mm. (b) Image with red fluorescent spheres. (c) Imaging with both green and red fluorescent spheres. (d)–(f) Corresponding intensity profiles along the lines in (a)–(c).

3.2. Two-color detections of zebrafish embryos

The flow-based two-color zebrafish sorting system enables the detection of the two-color fluorescent-labeled zebrafish embryos flowing through the capillary, as shown in Fig. 3. The brighter part of Fig. 3(a) with large gray values is the yolk sac of embryo, which has weak auto-fluorescence. The right part of Fig. 3(a) is the gray value distribution. Figure 3(b) shows an embryo with only green fluorescence marking its blood vessels. Here, the 488 nm channels have strong green fluorescent signals. In contrast, Fig. 3(c) shows an embryo with only red fluorescence. Strong fluorescence appeared at the 561 channels. Figure 3(d) shows an image of embryo simultaneously marked with two colors. Both 488 nm and 561 nm channels detected strong fluorescence, as expected. So, it is inferred that the gray values of the images with fluorescent marks are much larger than those without fluorescent marks, allowing us to sort zebrafish embryos according to the average value or standard deviation.

3.3. Determining the sorting threshold

In the previous section, the fluorescence intensity distributions of the four fishes were shown. To

determine the sorting threshold, a large number of zebrafish embryo images were collected by our system, and their mean and standard deviation were calculated. Figure 4 shows the average intensity and standard deviation of the zebrafish embryo images. As shown in Fig. 4(a), the average intensity of some embryos was 0 or close to 0 and the most of them was gather at 0.01–0.10. In Fig. 4(b), the average intensity of the wild-type embryos was 0 or close to 0, because the yolk sac of zebrafish can fluoresce spontaneously. Figures 4(c)–4(d) clearly shows difference in the distribution of the standard deviation between the fluorescent-labeled and the wild-type embryos. The standard deviation reflects the dispersion of a set of data from its average. The standard deviation of the fluorescent-labeled embryos was larger than the wild-type embryos. For the red fluorescent-labeled zebrafish embryo, the sorting threshold of average intensity was set to 0.002 or the sorting threshold of standard deviation was set to 0.05.

Figures 5(a)–5(b) shows the average intensity of the zebrafish embryo images with green fluorescent markers. The average fluorescence intensity of the embryos labeled with green fluorescence is larger than wild type. Figures 5(c)–5(d) shows the standard deviation distribution of the embryos. The standard deviation of the embryos with fluorescence

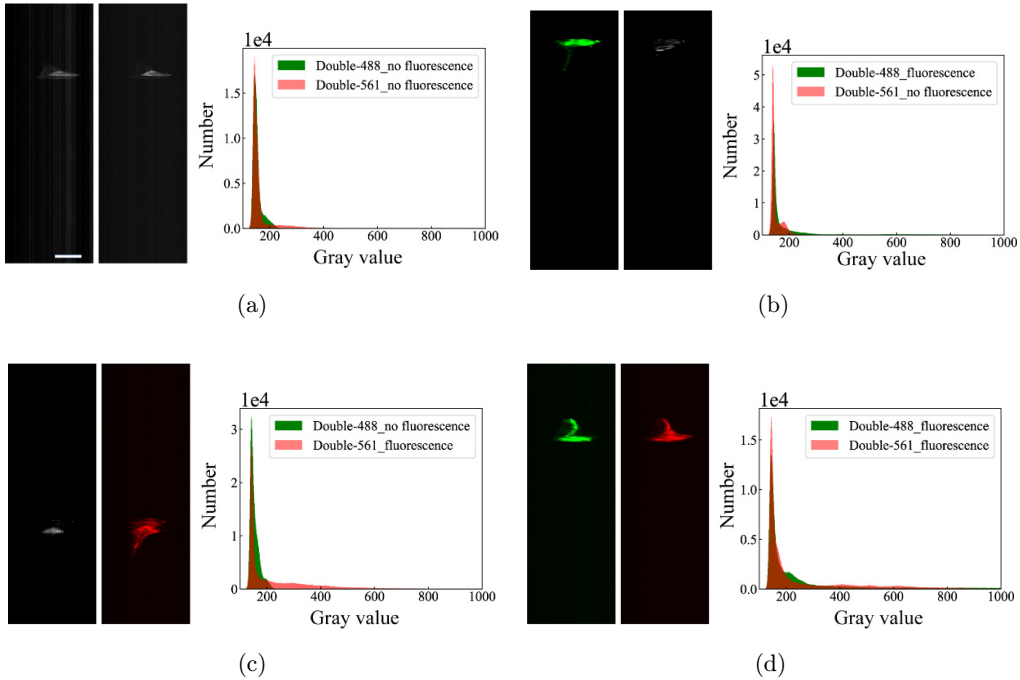


Fig. 3. Four different zebrafish embryo images captured using the two-color sorting system. (a) A wild-type zebrafish embryo (4 dpf) and its gray value distribution. Scale bar: 4 mm. (b) A zebrafish embryo with green fluorescent-labeled blood vessels. (c) A zebrafish embryo with red fluorescent-labeled blood cells. (d) A zebrafish embryo showing green and red fluorescent signals.

signals was generally higher than those without. For the green fluorescent-labeled zebrafish embryos, the sorting threshold of average intensity was set to 0.002 or the sorting threshold of standard deviation was set to 0.015.

3.4. Sorting mixed embryos

Our flow-based two-color zebrafish embryo sorting system is suitable for zebrafish embryos at 3–7 dpf.

Using our system, 80 embryos with two-color fluorescent markers, 84 embryos with red fluorescent markers, 82 embryos with green fluorescent markers, and 68 embryos without fluorescent markers were sorted according to fluorescence intensity. Figure 6 shows the number of correct and wrong sorting. At the end of sorting, the sorting results was observed by the stereoscope to obtain the accuracy of the sorting results. For the mixed embryos, our system can successfully sort

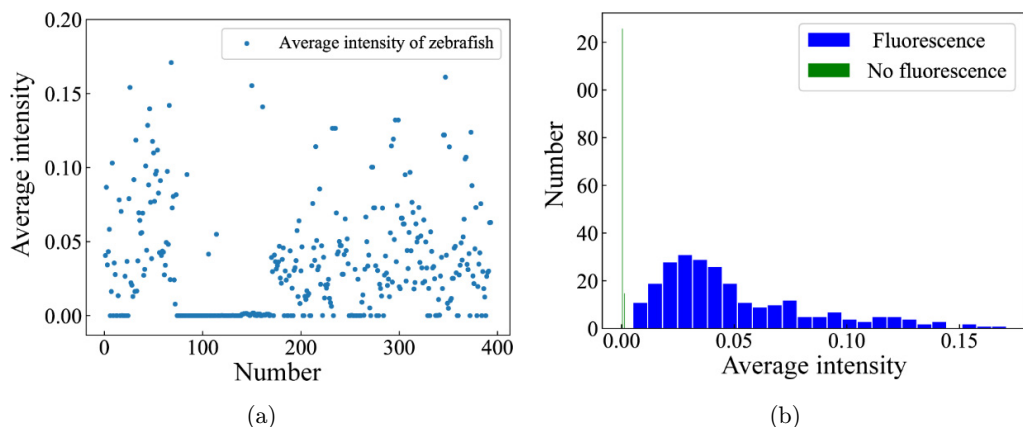


Fig. 4. The average intensity and standard deviation of the zebrafish embryo images with red fluorescent-labeled blood cells. (a) Average intensity distribution of the zebrafish embryos. (b) Histogram of the average fluorescence intensity of the embryos. (c) Standard deviation distribution of the zebrafish embryos. (d) Histogram of the standard deviation of the embryos.

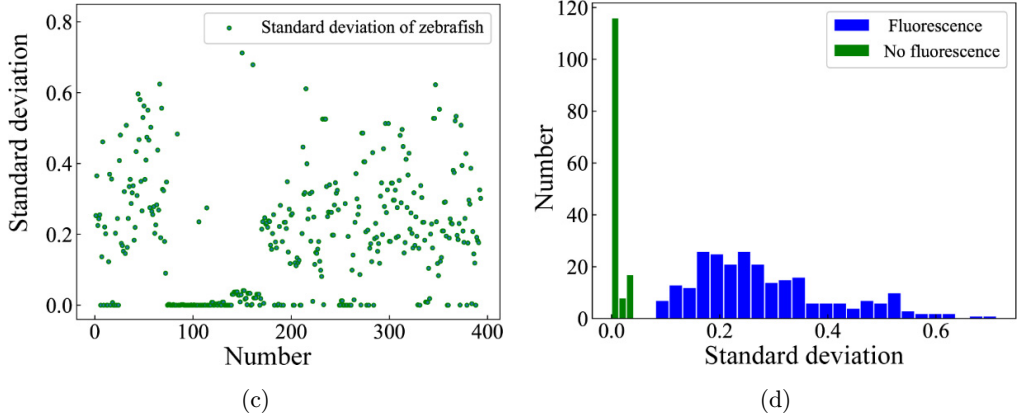


Fig. 4. (Continued)

zebrafish embryos with fluorescent markers with an accuracy higher than 95%. All 100 embryos survived after passing through our sorting system. However, five embryos of them died after 48 h.

They were possibly slightly injured during the sorting but could be not observed right away. The injury could be caused by the water flow or rubbing when passing the three-way valves. In the

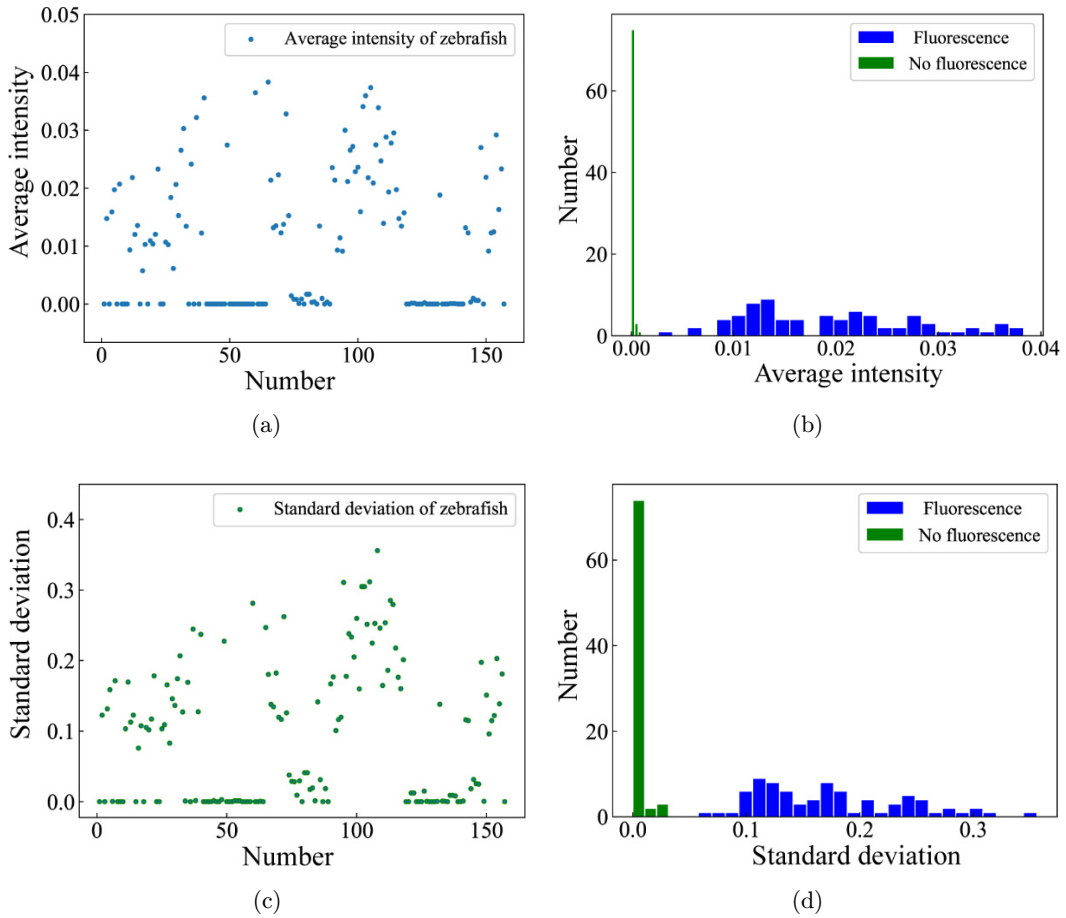


Fig. 5. The average intensity and standard deviation of the images of zebrafish embryos with green fluorescent-labeled blood vessels. (a) Average intensity distribution of the zebrafish embryos. (b) Histogram of the average intensity. (c) Standard deviation distribution of the embryos. (d) Histogram of the standard deviation.

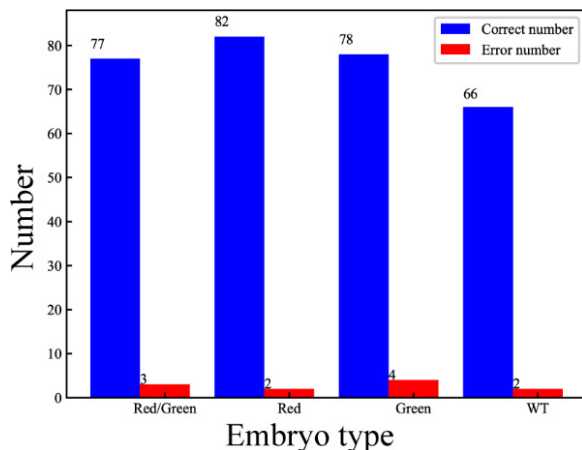


Fig. 6. Sorting accuracy of two-color-labeled zebrafish embryos.

future, we constitute to optimize the fluidics to improve the embryos' viability.

4. Conclusions

We developed a high-throughput sorting system for two-color fluorescence-labeled zebrafish embryos, which automatically loads and sorts the embryos. This system uses two-line imaging of an area array camera to capture the fluorescent signals of zebrafish embryos flowing through a capillary. The accuracy of the automatic sorting system was higher than 95%. Each embryo can be sorted within 20 s. With the listed optical, fluidical, and mechanical parts in the methods section, the sorting system can be easily built by most labs with instrumentation background. For labs focused on zebrafish research and application, there will be challenges on the optical alignment and control software. So in the future, we will continue to integrate the system into an easy-to-use, efficient and low-cost instrument for biological application. Our system has two detection channels, which can sort four classes, namely, green, red, green/red, and nonlabeled. In the future, the system can be upgraded to have additional detection channels to sort three- or four-colored label embryos.

Conflict of Interest

The authors declare no conflicts of interest related to this article.

Acknowledgments

We would like to thank the National Natural Science Foundation of China (No. 62205368), the Suzhou Basic Research Pilot Project (SJC2021013), the Key Research and Development Program of Jiangsu Province (BE2020664).

References

1. A. J. Hill, H. Teraoka, W. Heideman, R. E. Peterson, "Zebrafish as a model vertebrate for investigating chemical toxicity," *Toxicol. Sci.* **86**(1), 6–19 (2005).
2. E. Ellertsdóttir, A. Lenard, Y. Blum, A. Krudewig, L. Herwig, M. Affolter, H. G. Belting, "Vascular morphogenesis in the zebrafish embryo," *Dev. Biol.* **341**(1), 56–65 (2010).
3. J. F. Amatruda, J. L. Shepard, H. M. Stern, L. I. Zon, "Zebrafish as a cancer model system," *Cancer Cell* **1**(3), 229–231 (2002).
4. L. I. Zon and R. T. Peterson, "In vivo drug discovery in the zebrafish," *Nat. Rev. Drug Discov.* **4**(1), 35–44 (2005).
5. D. Li, X. Zhao, W. Qin, H. Zhang, Y. Fei, L. Liu, K. Yong, G. Chen, B. Z. Tang, J. Qian, "Toxicity assessment and long-term three-photon fluorescence imaging of bright aggregation-induced emission nanodots in zebrafish," *Nano Res.* **9**(7), 1921–1933 (2016).
6. N. D. Meeker and N. S. Trede, "Immunology and zebrafish: Spawning new models of human disease," *Dev. Comp. Immunol.* **32**(7), 745–757 (2008).
7. T. Y. Chang, C. Pardo-Martin, A. Allalou, C. Wählby, M. F. Yanik, "Fully automated cellular-resolution vertebrate sorting platform with parallel animal processing," *Lab Chip* **12**(4), 711–716 (2012).
8. S. F. Graf, S. Hötzl, U. Liebel, A. Stemmer, H. F. Knapp, "Image-based fluidic sorting system for automated zebrafish egg sorting into multiwell plates," *J. Lab. Autom.* **16**(2), 105–111 (2011).
9. H. Breitwieser, M. Thomas, M. Vogt Ferg, C. Pylatiuk, "Fully automated pipetting sorting system for different morphological phenotypes of zebrafish embryos," *SLAS Technol., Transl. Life Sci. Innov.* **23**(2), 128–133 (2017).
10. A. Vogt, A. Cholewiński, X. Shen, S. G. Nelson, J. S. Lazo, M. Tsang, N. A. Hukriede, "Automated image-based phenotypic analysis in zebrafish embryos," *Dev. Dyn.* **238**(3), 656–663 (2009).
11. Y. Guo, W. J. Veneman, H. P. Spaink, F. J. Verbeek, "Three-dimensional reconstruction and measurements of zebrafish larvae from high-throughput

- axial-view in vivo imaging,” *Biomed. Opt. Express* **8**(5), 2611–2634 (2017).
- 12. I. Lee, J. Hsu, Y. Chuang, I. Liau, “Confocal imaging guided photochemical thrombosis toward the development of a novel zebrafish model of stroke,” *2016 Asia Communications and Photonics Conf.*, pp. 1–3, IEEE (2016).
 - 13. W. Yang, W. Wang, L. Jing, S.-L. Chen, “Label-free photoacoustic microscopy: A potential tool for the live imaging of blood disorders in zebrafish,” *Biomed. Opt. Express* **12**(6), 3643–3649 (2021).
 - 14. A. Pfriem, C. Pylatiuk, R. Alshut, B. Ziegner, S. Schulz, G. Brethauer, “A modular, low-cost robot for zebrafish handling,” *2012 Annual Int. Conf. IEEE Engineering in Medicine and Biology Society*, pp. 980–983, IEEE (2012).
 - 15. E. J. Gualda, H. Pereira, T. Vale, M. F. Estrada, C. Brito, N. Moreno, “SPIM-fluid: Open source light-sheet-based platform for high-throughput imaging,” *Biomed. Opt. Express* **6**(11), 4447–4456 (2015).
 - 16. P. J. Keller, A. D. Schmidt, J. Wittbrodt, E. H. K. Stelzer, “Reconstruction of zebrafish early embryonic development by scanned light sheet microscopy,” *Science* **322**(5904), 1065–1069 (2008).
 - 17. T. V. Truong, W. Supatto, D. S. Koos, J. M. Choi, S. E. Fraser, “Deep and fast live imaging with two-photon scanned light-sheet microscopy,” *Nat. Methods* **8**(9), 757–760 (2011).
 - 18. M. Weber and J. Huisken, “Light sheet microscopy for real-time developmental biology,” *Curr. Opin. Genet. Dev.* **21**(5), 566–572 (2011).
 - 19. C. Pardo-Martin, T.-Y. Chang, B. K. Koo, C. L. Gilleland, S. C. Wasserman, M. F. Yanik, “High-throughput in vivo vertebrate screening,” *Nat. Methods* **7**(8), 634–636 (2010).
 - 20. S. Takanezawa, T. Saitou, T. Imamura, “Wide field light-sheet microscopy with lens-axicon controlled two-photon Bessel beam illumination,” *Nat. Commun.* **12**(1), 2979 (2021).